Study of an Electron Magnetohydrodynamic Flow of Iron Oxide Nanofluid under the Impacts of Heat Generation/Absorption

Abdullahi Madaki Gamsha [*], Rozaini Roslan[†], Muhammad Ghazali Kamardan[‡], Aminu Barde[§], Mohammed Kamalrulzaman Mohd Akhir[**]

Abstract

This study is primarily concerned with the heat transmission properties of the Fe_3O_4- water base nanofluid, as it flows across an exponentially impermeable shrinking/stretching surface. The proposed study examines how a boundary layer fluid flow toward a shrinking/stretching surface is affected by an electric field, heat generation/absorption, and surface impermeability. Partial differential equations (PDEs) are used to illustrate the sense of flow. Using the proper similarity transformation technique, the PDEs are converted into the system of ODEs. The firing process is then applied to these altered equations. The study shows that the momentum profile fluctuates by increasing the values of variable viscosity parameter, while intensified by varying electricity, and magnetic field parameters. The converse happens when the impermeability parameter is increased. The temperature profile is also improved by an increase in heat absorption and magnetic field parameters. On the Nusselt number profile: The Prandtl number increases the Nusselt number whereas, the mixed convection parameter decreases the Nusselt number of the system. The results may be useful in various technical domains, including optimizing the petroleum pipeline flow. The findings can help direct further research in this field and advance our understanding of heat and mass transmission mechanisms.

Keyword: Heat Generation/Absorption, Electric Field, Suction/Injection, Magnetic Field, Nanofluid.

Introduction

By dispersion of nanometer-sized particles (nanoparticles, nanofibers, nanotubes, nanowires, nanorods, nanosheets, or droplets) in base fluids, nanofluids are a revolutionary way to break up fluids. To put it another way, nanofluids are colloidal suspensions at the nanoscale that

[*]Corresponding Author: Department of Mathematical Sciences, Abubakar Tafawa Balewa University, PMB 0248, Bauchi. Nigeria, agmadaki@atbu.edu.ng

[†]Department of Mathematics and Statistics, Faculty of Applied Sciences and Technology, University Tun Hussein Onn Malaysia, Pagoh Campus, Muar 84600, Johor, Malaysia, rozaini@uthm.edu.my

[‡]Department of Mathematics and Statistics, Faculty of Applied Sciences and Technology, University Tun Hussein Onn Malaysia, Pagoh Campus, Muar 84600, Johor, Malaysia, mghazali@uthm.edu.my

[§]Department of Mathematical Sciences, Abubakar Tafawa Balewa University, PMB 0248, Bauchi. Nigeria, bardealamin@yahoo.com

[**]Department of Electrical Engineering Technology, Faculty of Engineering Technology, University Tum Hussein Onn Malaysia, Pagoh Campus, Muar 84600, Johor, Malaysia, mkamarul@uthm.edu.my

contain diluted nanomaterials. There are two-phase systems, one of which is associated with the liquid phase and the other with the solid phase as discussed by Wu et al (2019). When compared to base fluids like water or oil, nanofluids have been developed to have better thermophysical characteristics, including convective heat transfer coefficients, viscosity, thermal conductivity, and thermal diffusivity. It is well-established by Sundaram and Sowndharya (2025) and explains its wide range of potential uses. The goal of developing nanofluids is to reduce the size of heat transfer equipment by using them as thermo-fluids in heat exchangers to increase the heat transfer coefficient.

The features of nanofluids, such as density, specific heat, viscosity, and thermal conductivity, are crucial factors that affect their heat transmission characteristics. The operating temperature of nanofluids affects their thermophysical characteristics as well. Therefore, it is crucial to evaluate the temperature-dependent characteristics of nanofluids precisely. In many manufacturing processes, including power generation, heating or cooling, chemical reactions, and microelectronics, common fluids like water, ethylene glycol, and heat transfer oil are essential. However, because of their relatively low thermal conductivity, these fluids are unable to achieve high heat substitution rates in thermal engineering systems.

Using ultra-fine solid particles balanced in numerous fluids to increase their heat conductivity is one method to overcome this impermeability. A nanofluid is a mixture of nanoparticles (1–100 nm) suspended in a regular base fluid. Choi (1995) coined the term "nanofluid." When compared to suspensions containing millimetre- or micrometre-sized particles, nanofluids exhibit superior stability, rheological characteristics, and significantly higher thermal conductivities.

Nanoscale materials having unique magnetic properties are known as magnetic nanoparticles (MNPs), and they have been widely used in many different industries Cardoso et al. (2018), Ali et al. (2021), Oyelami et al. (2023). MNPs are now at the forefront of Nano-science and Nanobiotechnology due to their quick development and an unparalleled volume of research Ahmadi et al. (2021), Dash et al. (2022). Size control, particle surface effects, and dipolar interactions are some of the key challenges in the production of monodisperse magnetic nanostructures. However, limiting the nucleation and spread of such MNPs has become easier because it improves chemical production techniques. According to Hussaini et al. (2024), MNPs are made up of either multiple metallic materials or their magnetic oxides and composites. Superparamagnetic magnetite (Fe_3O_4) is the most widely used iron oxide or magnetic oxide because of its high surface area, low toxicity, and excellent biocompatibility (Elsayed et al., 2023; Zamani and Stadler, 2020). Moreover, the three most common iron oxides in nature are magnetite (Fe_3O_4), hematite (α-Fe_2O_3), and maghemite (γ-Fe_2O_3). In the fields of science and technology, these oxides are extremely important, Sun et al. (2020), Liu et al. (2020).

The impacts of thermal Marangoni convective magneto-Casson fluid flow through the suspension of nanoparticles are examined by Mahanthesh et al. (2018), who considered the surface tension to be fluctuating linearly with temperature. The purpose of heat generation/absorption is to decrease/ increase a fluid's thermal conductivity, correspondingly. The temperature of the high-conductivity fluid rises, while the low-conductivity fluid exhibits the reverse behaviour as discussed by Noor et al. (2021). Using the power series technique, Qasim (2013) examined the effects of heat generation/ absorption around the temperature and mass movement on a vertical stretching plate.

Furthermore, Madaki et al (2024d) discussed extensively the heat and mass transfer along heat transmission of the MHD composite nanofluid through the squeezing of a pair of parallel plates acting as thermal radiation sources, with vanadium pentoxide (V_2O_5) acting as the solid material (nanoparticle). Squeezing Jeffrey's hybrid nanofluid flow due to its complexity in terms of governing equations. Therefore, their research is aimed at obtaining the mathematical solutions of the Mass and heat transfer in radiant-MHD vanadium pentoxide (V_2O_5)-based squeezing flow Jeffrey nanofluid hybrids which are equipped with heat generation/ absorption.

The prime goal of Hussaini et al. (2023) is to analyze the effect of heat generation/absorption on an existing mathematical model. Asghar et al. (2023) investigated the consequence of heat generation along with absorption as well as the slip velocity by carrying out a vertically shrinking sheet. A 2-dimensional magnetic nanofluid is looked at numerically for convection. They explored an Al_2O_3– Cu/water composite nanofluid, where water serves as the base liquid and copper (Cu) and alumina Al_2O_3 serve as the solid nanoparticles. These days, composite nanofluids improve heat transmission efficiency. Using the Tiwari-Das model, they examined the effects of heat generation/absorption, MHD, mixed convection, velocity slip parameters, and the solid volume fraction of copper on temperature and velocity distributions. Abo-Dahab et al. (2023) examined the mathematical projections of the double-diffusive peristaltic descend of a non-Newtonian Sisko nanofluid across a porous medium beneath a longitudinally asymmetrical flexible channel within the impact of heating by Joule, non-linear thermal radiation, viscous dissipation, and heat generation/absorption in the presence of heat and mass convection, taking into account the effects of Brownian motion and the thermophoresis coefficients. The impact of heat generation and absorption on MHD nanofluid flow across a stretching surface is examined by Hussaini (2022). He also went into great detail on how other factors affect the profiles of temperature, momentum, concentration of nanoparticles, and Nusselt number. He concentrated his research on the impact of sun radiation, magnetic fields, heat creation and absorption, and other factors.

The computational research intended to investigate the impact of copper and alumina on the flow of an engine oil-based nanofluid through a Darcy–Forchheimer porous medium is covered in detail by Rasool et al. (2024). With consideration for the effects of Brownian motion and the thermophoresis coefficients. The ultimate findings showed that as the Forchheimer number expands, the velocity diminishes due to the inertial effect included in the flow model. More importantly, the velocity profile is enhanced by the larger volume proportion of both kinds of nanoparticles. The volume fraction has a significant impact on the temperature. Greater heat flow is produced by a convective border and a higher Biot number than by a non-convective barrier. Interesting streamlines and contour graphs are created for two specific examples, both with and without the magnetohydrodynamic effect.

However, a numerical investigation is conducted by Bendjaghlouli et al. (2024) to explore the influence of the magnetic field and the electric conductivity of container walls on the swirling flow of a hybrid nanofluid. In this study, a stationary inner wall and a rotating outer wall with a fixed Ω are considered within the annular between coaxial cylinders. Radial application of a magnetic field is utilized to assess its impact on the average Nusselt number. The mathematical model, formulated by differential equations, is solved using the finite volume method. The study examined the variations in azimuthal velocity, temperature, and Nusselt number with increasing magnetic intensity. The Darcy-Forchheimer phenomena and heat transport in unbalanced magnetohydrodynamics (MHD) flow have been explored by Waheed et al. (2024). The system incorporates a Casson nanofluid (CNF), with heat transfer during melting and slip velocity dictated by heat source/sink and thermal radiation.

The examination of the current problem is motivated by the practical physics squeeze flow. In a mathematical process, nonlinear partial differential equations (PDEs) are transformed into nonlinear ordinary differential equations (ODEs). Using the Homotopy perturbation technique (HPM) and taking into account the proper boundary conditions (BCs), the nonlinear ODEs are solved analytically. A large number of dimensionless physical quantities are obtained by a non-dimensional process. The primary outcomes of velocity, temperature profiles, local skin-friction, and the local Nusselt number have been assessed and displayed through a number of non-dimensional parameters.

Khadija et al. (2013) aim to investigate entropy production on viscous $TiO_2{-}C_2H_6O_2$ nanofluid across a porous medium with a permeable exponential surface, causing the aggregation of nanoparticles with heat radiation and mixed convective stagnation point flow. A suitable similarity transformation is used to simplify the controlling partial differential equations, producing a set of ordinary differential equations. They employed fourth-order Runge-Kutta integration and Mathematica's shooting approach to provide a numerical solution to these equations. Mahmood et al. (2023) ascertain how NP shape affects the entropy generated by $Al_2O_3{-}H_2O$ nanofluid along a porous MHD stretched sheet with heat radiation, viscous dissipation, and quadratic velocity H_2O as frozen fluid, on the other hand, $Al_2O_3{-}H_2O$ nanofluid, among five various NP forms (oblate spheroid, platelet, blade, brick, and cylinder), is the hot fluid. Nanofluid containing $Al_2O_3{-}H_2O$ is widely used in industrial production due to its exceptional ability to increase heat transmission. The governing PDEs are transformed into a nonlinear differential system of connected ODEs using a series of similarity transformations.

The enormous uses of Electron Magnetohydrodynamic (EMHD) in machine building and industry are covered by Madaki et al. (2023). Magnetohydrodynamic fluid flow through a stretched sheet with non-linear thickness variations is the basis of their study. It also incorporates the electric field. Water is regarded as the base fluid, and inside it is copper (Cu) nanoparticles that are nanometers in size. Their primary concern is the impact of certain relevant variables on the model, including chemical reactions, induction heat, Dufour diffusivity, Joule heating, variable fluid viscosity, surface impermeability, non-uniform heat flux, and viscous dissipation, among other parameters.

As is readily apparent from the previously scrutinized literature, the primary objective of this work is to examine the properties of mixed convective nanofluid flow over an impermeable exponential shrinking/stretching surface with heat generation/absorption effects and the suction/injection parameters. The standard base fluid is water that contains solid Fe_3O_4 nanoparticles. The temperature and velocity profiles are derived from the numerical data. The current findings are in line with those of Kumar et al. (2023), who previously published their work. Additional pertinent studies in this field are Wakif et al. (2024), and Helen et al. (2024). A review of the literature indicates that no such studies have been published to date that support the aforementioned effects. It is anticipated that the current study helps novice researchers understand the thermal and dynamical properties of nanofluid.

Mathematical Analysis

A continuous flow of a fluid that resembles a velocipede across a stretching/shrinking sheet is taken into consideration, and the momentum, temperature and Nusselt number of the entire surface are kept constant. The fluid has a temperature of T_∞ at the open channels. A uniform first-order reaction with a steady pace represented by kc, is responsible for the chemical interaction between the liquid and the diffusing components.

It is thought that the fluid's characteristics never change. A magnetic field and electric field are induced by taking a weak magnetic Reynolds number. They are continually applied at maximal intensity. Viscous dissipation is expected to have a major effect. The surface temperature of the stretching/shrinking sheet is thought to fluctuate, as seen in Figure 1 below. Assuming the boundary layer approximation is valid, the following are the governing equations for the Boussinesq approximation.

$$\frac{\partial u}{\partial x} + \frac{\partial v}{\partial y} = 0, \tag{1}$$

$$u\frac{\partial u}{\partial x} + v\frac{\partial v}{\partial y} = \frac{1}{\rho_{nf}}\left[\begin{array}{l}\mu_{nf}\dfrac{\partial^2 u}{\partial y^2} - \sigma_{nf}(E(x)B_0(x) - \\ B_0(x)^2 u) + g(\rho\beta)_{nf}(T - T_\infty)\end{array}\right] + \frac{\mu_e}{k}u, \tag{2}$$

$$(\rho Cp)_{nf}\left(u\frac{\partial T}{\partial x} + v\frac{\partial T}{\partial y}\right) = \left(k_{nf} + \frac{16T_\infty^3\sigma}{3k_f k_f^*}\right)\frac{\partial^2 T}{\partial y^2}$$
$$+\sigma_{nf}(uB_0(x) - E(x))^2 + \frac{Q}{\rho_{nf}}(T - T_\infty), \tag{3}$$

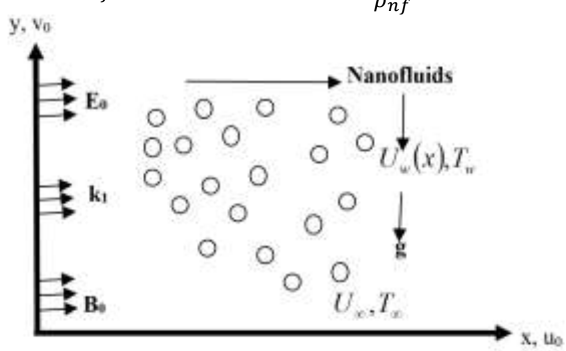

Figure 1: The physical model of the problem.

The constraints are stated as follow:

$$u = \lambda_1 u_w(x) + A_1\frac{du}{dy},\ v = v_w(x),\ T = T_w(x)\ at\ y = 0,$$

$$u = 0,\ T = T_\infty\ as\ y \to \infty \tag{4}$$

In this case, the fluid density is represented by $\rho_{nf} = (1-\phi)_{\rho f} + \phi_{\rho s}\rho$, $\mu_{nf} = \frac{\mu_f}{(1-\phi)^{2.5}}$ is the dynamic viscosity, $\sigma_{nf} = 1 + \frac{3\phi\left(\frac{\sigma_s}{\sigma_f}-1\right)}{\left(\frac{\sigma_s}{\sigma_f}+2\right)-\left(\frac{\sigma_s}{\sigma_f}-1\right)}\sigma_f$ denotes the electric conductivity, $\alpha_{nf} = \frac{k_{nf}}{(\rho Cp)_{nf}}$ denotes the thermal conductivity of the fluid, $(\rho\beta)_{nf}$ represents the thermal expansion of nanofluid, and $\frac{\mu_e}{k}u$ stands for impermeability of the stretching/shrinking surface. $(\rho Cp)_{nf}$ is the nanofluid heat capacitance, is the Q is the radiative heat transfer, $\lambda = \frac{Q}{(\rho Cp)_{nf}T_w\rho_{nf}}$ is the heat generation/absorption parameter, T is the fluid's temperature. In addition, u and v represent the fluid's velocities in the x and y directions, while B_0 represents the magnetic field. The coefficient of chemical interactions is shown by k_c, and the heat at the free stream is indicated by T_∞, the wall's heat is indicated by T_w. Assuming that the surface temperature varies in the manner described below.

$$T_w(x) - T_\infty = Ax^n. \tag{5}$$

The momentum $f(\eta)$ and temperature $\theta(\eta)$ are used as a stream term ψ and a similarity term η

$$\begin{gathered}\eta = y\sqrt{\frac{U_w}{2\vartheta L}}e^{x/2L}, \psi = \sqrt{2\vartheta L u_w}\,e^{x/2L} f(\eta),\\ \theta(\eta) = \frac{T-T_\infty}{T_w-T_\infty}.\end{gathered} \tag{6}$$

Here, $\psi(x, y)$ denotes stream function that is demarcated into

$$u = \frac{\partial\psi}{\partial y} = Uf'\text{and } v = -\frac{\partial\psi}{\partial x} = \frac{1}{2}\sqrt{\frac{uv}{x}}\left(\eta f' - f\right). \tag{7}$$

It is noteworthy that prime denotes differentiation about η.

The following is the result of reducing Equations (1) to Eq. (4) using Equations (5) to (7):

$$f''' + (1-\phi)^{2.5}\left\{\begin{matrix}(1-\phi) + \phi\left(\frac{\rho_s}{\rho_f}\right)\left(-2f'^2 + f''f\right)\\ -2\left(1 + \frac{3\phi\left(\frac{\sigma_s}{\sigma_f}-1\right)}{\left(\frac{\sigma_s}{\sigma_f}+2\right)-\left(\frac{\sigma_s}{\sigma_f}-1\right)\phi}\sigma_f\right)\\ (A_2M(E_1 - f')) - k_1f'\end{matrix}\right\} = 0, \tag{8}$$

$$\left(\frac{k_{nf}}{k_f} + \frac{4}{3}Rd\right)\theta'' + Pr\left\{(1-\phi) + \phi\frac{(\rho Cp)_s}{(\rho Cp)_f}\left(f\theta' - 4f'\theta\right)\right\}$$

$$+A_2EcM\left(f^{'}-E_1\right)^2+\lambda\theta=0, \tag{9}$$

The following boundary conditions apply:

$$f^{'}(0)=\lambda_1, f(0)=S, \theta(0)=\delta(1-\theta(0))$$
$$f^{'}(\infty)=0, \theta^{'}(\infty)=0. \tag{10}$$

In addition, $A_2=2\vartheta U_w(T_w-T_\infty)$ is the variable viscosity parameter, $M=\frac{\sigma B_0^2L}{\rho U_w}$ is the magnetic field, $E_1=\frac{2LE_0}{\sigma B_0^2U_w}$ is the electric field parameter, $k_1=\frac{2LU_w\mu_e}{k}$ represents the dimensionless impermeability parameter, $Rd=\frac{4T_\infty^3\sigma^*}{k_fk_f^*}$ stands as the non-dimensional radiation parameter, $Pr=\frac{\vartheta(\rho Cp)_f}{k_f}$ is the Prandtl number, $Ec=\frac{U_w^2}{\vartheta(T_w(x)-T_\infty)}$ stands for the total amount of Eckert number and $\lambda=\frac{\vartheta Q}{U_wT_w\rho_{nf}}$ is the heat generation/ absorption parameter. The suction/injection parameter is given by $S=-\sqrt{\frac{2L}{\vartheta U_w}}$, $\lambda_1=A\sqrt{\frac{\vartheta U_w}{2L}}$ is the stretching/ shrinking parameter, while $\delta=B\sqrt{\frac{U_w}{2\vartheta L}}$ is the thermal slip parameter.

Numerical Results and Discussion

Maple software uses the shooting technique to provide mathematical responses to mathematical Equations 2 and 3. By considering various initial estimations for shrinking and stretching instances of the surface, this software automatically uses the fourth-fifth order Runge-Kutta-Fehlberg technique to solve boundary value problems numerically. The physical characteristics of the solid nanoparticles (Fe_3O_4) and the base fluid water are shown numerically in Table 1. Numerical comparisons are made between the present results and previously obtained results for accuracy and robustness, which are available at Kumar et al. (2023) and Meade et al. (1996). There is good agreement between these numerical results (see Table 2).

Additionally, the temperature and velocity profiles are obtained at various physical parameter values. However, Figures 2–7 display the computed numerical results to clarify the silent aspects with respect to the existence of various flow characteristics used in velocity, thermal energy transmission, mathematical equations, and the Nusselt number profiles. It is commonly known that any external forces affecting the fluid's motion directly affect the axial velocity of the fluid moving within the channel. Figure 2 shows the variation of momentum under the influence of the varying viscosity parameter.

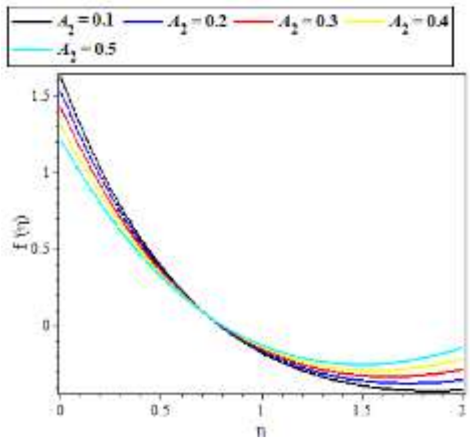

Figure 2: Influence of Variable Viscosity parameter on momentum profile.

These outside factors have the potential to modify the pace, either increasing or decreasing, on the other hand, creating an erratic velocity. In addition, Figure 2 illustrates how the axial velocity distribution is affected by the variable viscosity parameter. This can easily be seen from a close examination of the figure the disorganized behaviors of the axial velocity distribution, between increases and drops inside the channel under this parameter's effect. The velocity distribution decreases on the left-hand side of the graph but increases on the right-hand side of the graph. However, physically, when a fluid experiences resistance when passing through a porous media, it is thought to be one of the external forces at play. Although a drop in velocity is expected inside the channel generally, there are variations in the axial velocity distribution within the medium due to variations in the density and thickness of specific areas of the porous medium inside the channel. The main reason for the variance in the longitudinal velocity dispersion is that the higher and thinner pores had a relatively large velocity, while the velocity through the thicker and denser porous medium is modest. On the other hand, the effects of electricity (E1) on the momentum profile as illustrated in Figure 3 which examines how the parameter decreases the momentum of the system. Substantially, the fluid movement inside the channel is forced to move in the opposite direction by the electricity parameter, which produces a resistance force. The Lorentz force is the term used for this force. Usually, this force weakens and reduces the fluid's velocity; however, in a region of the fluid where a decrease is seen, this force intensifies. In other places, its speed vanishes, and as a result, velocity rises. In the distribution of axial velocity, this is aberrant behavior. Furthermore, a closer look at Figure 4 shows that the temperature distribution is rising together with the enhancement of the heat absorption parameter $(\lambda < 0)$. On the other hand, an increase in the heat generation parameter values $(\lambda > 0)$ shows the opposite trend.

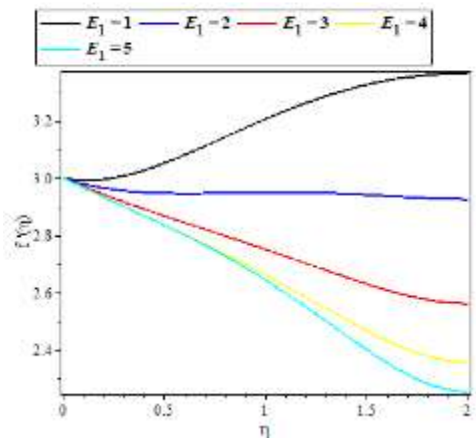

Figure 3: Influence of Electricity parameter on momentum profile

This is because temperature influences the kinetic energy involved in the movement of fluid molecules and nanoparticles, as well as creating tiny gaps between the fluid molecules, the average kinetic energy of the fluid particles physically causes an increase in the temperature distribution field transit of heat absorption. Which increases the movement and speed of the fluid molecules within the channel. Similarly, Figure 5 shows the temperature variation under the influence of the magnetic field (M); it can be observed that the temperature distribution for both the ground fluid and the nanofluid is enhanced by an increase in the parameter's values.

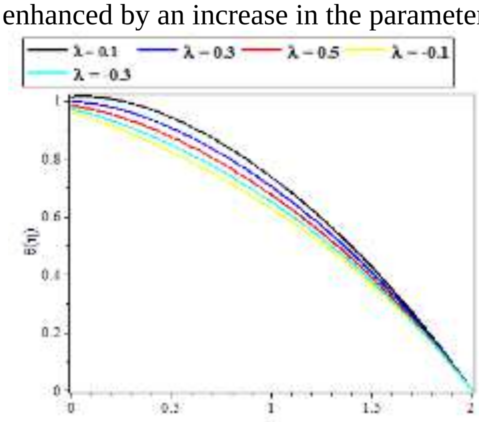

Figure 4: Influence of heat generation/ absorption on temperature profile

One possible explanation for this result is that the higher magnetic field value improves heat dissipation through radiative processes, which affects the fluid's thermal energy and in turn, its temperature distribution. Moreover, Figure 6 is plotted to explain the effect of the Prandtl number parameter (Pr) over the local Nusselt number profile.

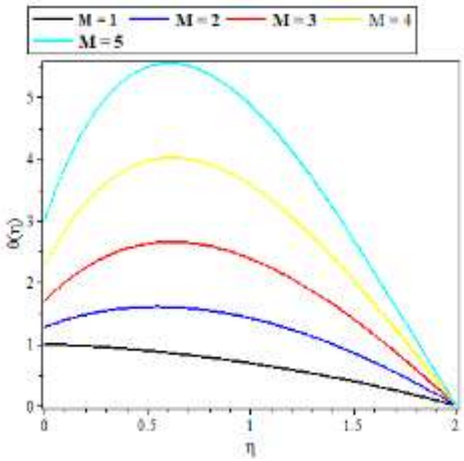

Figure 5: Influence of magnetic parameter on temperature profile

Here it is studied that any increment in the values of the parameter brings about a decrease in skin friction coefficient and a reverse for the case of the local Nusselt number profile. Tangibly, this seems to be reasonable. It's noteworthy to notice that for the Prandtl number parameter, the local Nusselt number for the fluid in the presence of nanoparticles is larger than the fluid in its absence. Consequently, the influence of the mixed convection parameter (ξ) on the Nusselt number profile is depicted in Figure 7. The profile of the Nusselt number behaves erratically as the parameter increases. The Nusselt number exhibits extemporaneous comportment. The presence of hot air close to the powder could potentially be a contributing factor. The Nusselt number profile is heightened by the mixed convection parameter when the external temperature is zero.

However, this plot displays the fluctuation of the Nusselt number profile with mixed convection parameter (ξ). While the fluid's temperature and velocity do not significantly change when the mixed convection parameter (ξ) grows, it is noticed that an increase in the mixed convection parameter (ξ) value decreases the Nusselt number of species in the boundary layer. Owing to this, the mixed convection parameter (ξ) in this system induces the chemical to be absorbed, which lowers the Nusselt number profile. The primary outcome is that the first-order chemical reaction leans to reduce overshoot in the Nusselt Number profile in the solutal border layer.

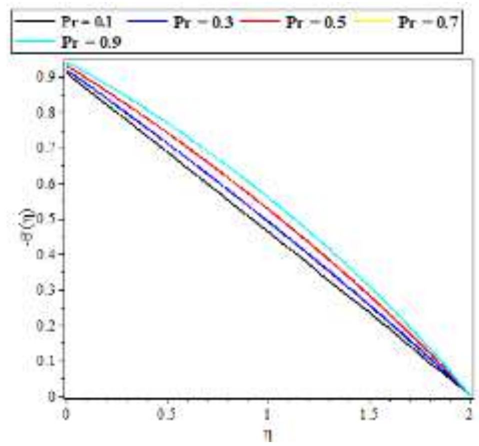

Figure 6: Influence of Prandtl number on Nusselt number profile

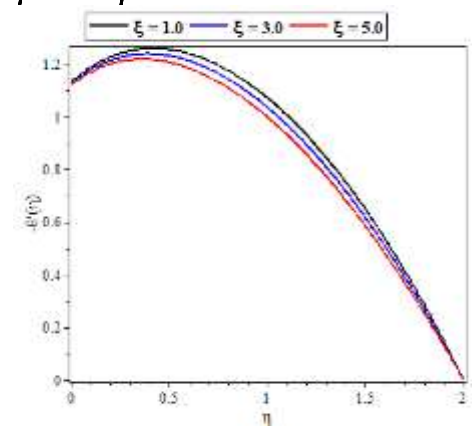

Figure 7: Influence of mixed convection parameter on Nusselt number profile

Table 1: list of thermophysical characteristics of certain nanoparticles and water (base fluid). Kumar et al. (2023)

	$\rho(kgm^{-3})$	$Cp(kg^{-1}k^{-1})$	$k(Wm^{-1}k^{-1})$	$\beta \times 10^{-5}(k^{-1})$
Water	997.1	4179	0.6130	21.0
Fe_3O_4	5180	670	80.4	20.6

Table 2: Values in comparison of $f''(0)$ and $-\theta'(0)$ with published results of Kumar et al. (2023).

Varying parameter	Kumar et al. (2023)		Present result	
S	$f''(0)$	$-\theta'(0)$	$f''(0)$	$-\theta'(0)$
0	1.28181	0.767768	1.28181	0.767766
0.3	-	-	1.38501	0.896891
0.6	1.5982	1.014571	1.59828	1.014580
0.8	-	-	1.70173	1.732067
1.0	-	-	1.98016	2.497629

Conclusion

The heat and mass transfer of a Fe_3O_4-water base nanofluid on a stretching/shrinking surface, along with the heat generation/absorption parameter and the surface impermeability, is investigated numerically in a mixed convection EMHD boundary layer laminar flow. Partial differential equations are changed into a set of ordinary differential equations to solve the current situation. Using the shooting strategy, the Maple software (in its default settings) finds and solves the similarity solution to the governing ordinary differential equations. Table 2 compares the numerically determined values of skin friction coefficients and local Nusselt numbers to validate the results. Additionally, the following conclusions are drawn from numerical observations of several physical parameters:

- The Momentum profile is irregular with the increase in variable viscosity. Otherwise, decreases with an increase in electricity parameter.
- Heat absorption parameters enhance the temperature of the system. However, as seen with the magnetic field parameter and heat generation, the contrary is the case.
- The Nusselt number profile is an increasing function with an increase in Prandtl number while mixed convection parameters decrease the Nusselt number of the system.

In conclusion, the present study has not only filled a significant knowledge vacuum regarding the boundary layer flow involving heat generation/ absorption and impermeability effects, but it also has promise for future use in a range of scientific and technical fields. By taking into account the impacts of chemical reactions or diffusion effects, the results direct future studies and add to the body of knowledge in the field of heat and mass transfer. It also provides workable answers for streamlining industrial procedures and fluid flow systems.

Table 4: Nomenclature.

x, y	Cartesian Coordinate
u, v	Components of velocities in the x and y-axes.
T	Temperature
$\boldsymbol{T_\infty}$	Ambient fluid temperature
θ	Dimensionless temperature
$\boldsymbol{C_p}$	Specific heat at the constant temperature
$\boldsymbol{\rho_{nf}}$	Density of nanofluid
$\boldsymbol{k_{nf}}$	Thermal conductivity of nanofluid
$\boldsymbol{\alpha_{nf}}$	Thermal diffusivity of nanofluid
$\boldsymbol{\sigma_{nf}}$	Electrical conductivity of the nanofluid
$(\boldsymbol{\rho C p})_{\boldsymbol{f}}$	Fluid heat capacitance
$(\boldsymbol{\rho C p})_{\boldsymbol{s}}$	Solid heat capacitance
$(\boldsymbol{\rho C p})_{\boldsymbol{nf}}$	Nanofluid heat capacitance
$(\boldsymbol{\rho \beta})_{\boldsymbol{nf}}$	Heat expansion of the nanofluid

μ_{nf}	Dynamic viscosity of nanofluid
η	Transformed variable
Fe_3O_4	Iron oxide
B_0	Magnetic field strength
ψ	Stream function
Pr	Prandtl number
U_w	Velocity of the nanofluid at the wall
λ	Heat generation/ absorption
λ_1	Stretching/shirking parameter
δ_T	Thermal slip parameter
R_{ex}	Local Remolds number
C_{fx}	Skin friction coefficient
N_{ux}	Nusselt number
Rd	Radiation parameter
S	Suction/ injection parameter
Δ	Velocity slip parameter
M	Magnetic parameter
k_1	Impermeability parameter
E_1	Electric field
g	Acceleration due to gravity
Q	Coefficient of heat generation

Conflict of Interest

Author (s) declare that they do not have any conflict of interest.

Funding Source

Authors received no funding support from a governmental nor non-governmental organization for the publication of this article.

Authors' Contributions

Each author made an equal contribution to the paper.

References

Abo-Dahab, S.M., Mohamed, R.A., Abd-Alla, A.M., Soliman, M.S. (2023) Double-diffusive peristaltic MHD Sisko nanofluid flow through a porous medium in presence of non-linear thermal radiation, heat generation/absorption, and Joule heating. *Scientific Reports.* 25;13(1):1432.

Ahmadi, M., Afkhami, A. & Madrakian, T. (2021). Magnetic Nanomaterials in Analytical Chemistry, *Elsevier B. V.: Amsterdam, the Netherlands*, pp. 1–354.

Ali, A., Shah, T., Ullah, R., Zhou, P., Guo, M., Ovais, M., Tan, Z., Y. & Rui, K. (2021). Review on Recent Progress in Magnetic Nanoparticles: Synthesis, Characterization, and Diverse Applications, *Front. Chem.* 9(629054).

Asghar, Adnan, Chandio, Abdul Fattah, Shah, Zahir, Vrinceanu, Narcisa, Deebani, Wejdan, Shutaywi, Meshal & Liaquat Ali Lund (2023). Magnetized mixed convection hybrid nanofluid with effect of heat generation/absorption and velocity slip condition, *Heliyon* Vol. 9 (13189).

Bendjaghlouli, Ali, Mahfoud, Brahim & Hibet Errahmane Mahfoud. (2024). Impact of wall electrical conductivity on heat transfer enhancement in MHD hybrid nanofluid flow within an annulus, *International Journal of Thermofluid Science and Technology*, 11(2), pp. 110204.

Cardoso, V.F., Francesko, A., Ribeiro, C., Bañobre-López, M., Martins, P., S. & Lanceros-Mendez. (2018). Advances in Magnetic nanoparticles for Biomedical Applications, *Advanced Healthcare Mater*, 7(1700845).

Choi, S.U.S. (1995). Enhancing thermal conductivity of fluids with nanoparticles, in: Developments and Applications of Non-Newtonian Flows, FED- vol. 231/MDvol. 66, pp. 99- 105.

Dash, S., Das, T., Patel, T. P., Panda, P. K., Suar, M. & Verma, S. K. (2022). Emerging trends in the nanomedicine applications of functionalized magnetic nanoparticles as novel therapies for acute and chronic diseases, *Journal of Nano biotechnology*, 20(393).

Elsayed, M. A., Elbashbeshy, M. F. & Khaled, M. A. (2023). Effects of chemical reaction and activation energy on Marangoni flow, heat and mass transfer over circular porous surface, *Arab Journal of Basic and Applied Sciences*, 30(1) 46- 54.

Hussaini, A. A., Madaki, A. G., Kabiru, S. A., Barde, A. & Abdullahi, I. (2022). Numerical approach for Convective magnetohydrodynamic (MHD) Nanofluid flow with impermeable stretching surface. *The Sciencetech.* (www.sciencetech.com). 3 (1), 1 – 16.

Hussaini, Abubakar Assidiq (2023). Magnetohydrodynamic (MHD) nanofluid flow over a non- linear stretchable Surface in the present of Heat generation/absorption. *International Journal of Scientific Research in Mathematics and Statistical Sciences, 10(6), 41- 50.*

Hussaini, A. A., Madaki, A. G. & Kwami, A. M. (2024). Modified Mathematical Model on the Study of Convective MHD Nanofluid flow with Heat Generation/Absorption, *International Journal of Engineering Research & Technology*, 10(09), 155-163.

Helen, O. F., Olumide, F. B., Olubunmi, I. E. & Yetunde, S. O. (2024). Numerical Study of Chemical Reaction and Magnetic Field Effects on MHD Boundary Layer Flow over a Flat Plate, *CFD Letters*, 16(3), 55-68.

Khadija, R., Zafar Mahmood, S. Saleem, Sayed M. Eldin & Umar K. (2024). Impact of nanoparticle shape on entropy production of nanofluid over permeable MHD stretching sheet at quadratic velocity and viscous dissipation, Case Studies in Thermal Engineering, 45, 102992.

Kumar, S., A. Shaikh, A., Shah, S. F., Lanjwani, H. B., Anwar, M. I. & Shehzad, S. A. (2023). Numerical investigation of magnetized thermally radiative Fe_3O_4-Water base nanofluid, *Chemical Physics Letters,* 824, 140571.

Liu, S., Yu, B., Wang, S., Shen, Y. & Cong, H. (2020). Preparation, urface functionalization and application of Fe_3O_4 magnetic nanoparticles, Advance Colloid Interface Science, 281, 102165.

Madaki, A. G., Hussaini, A. A., Alaramma, S. K., Musa, A. M., Tata, A. & A., Barde, A. (2023). Electron Magnetohydrodynamic (EMHD) Nanofluid flow with triple effects of Chemical reaction, Dufour diffusivity and impermeability of the surface along a slandering stretching sheet. *The Sciencetech*, *Vol.* 4, No 1, *pp. 23- 44*.

Madaki, A. G., Umar, A. B. & Hussaini, A. A. (2024d). Heat Source/Sink along Mass Suction Impacts on the Flow of the MHD Boundary layer across a Flat Plate, World Academics Journal of Engineering Sciences, 11(2).

Mahanthesh, B., Gireesha, B. & Animasaun, I. (2018). Exploration of Non-linear thermal Radiation and Suspended nanoparticles effects on mixed convection boundary layer flow of nanoliquids on a Melting Vertical Surface, *Journal of Nanofluids*, 7(5), 833- 843.

Mahmood, Zafar, Magda Abd El-Rahman, Umar Khan, Ahmed M Hassan & Hamiden Abd El-Wahed Khalifa. (2023). Entropy generation due to nanofluid flow in porous media over radiative permeable exponentially surface with nanoparticle aggregation effect. Tribology International, 188, 108852.

Meade, D.B., Haran, B.S., White, R.E. (1996). The shooting technique for the solution of two-point boundary value problems, *Maple Technical Newsletter*, 3 (1), 1–8.

Noor, N.A.M., Shafie, S. & Admon, M.A. (2021). Heat and mass transfer on MHD squeezing flow of Jeffrey nanofluid in horizontal channel through permeable medium, *PLoS One*, 16(5), e0250402.

Oyelami, F. H., Falodun, B. O., Ige, E. O. & Saka- Balogun, O. Y. (2023). Numerical Study of Chemical reaction and Magnetic field Effects on MHD Boundary Layer Flow over a Flat Plate, *CFD letters,* 16(3), 55-68.

Qasim, M. (2013). Heat and mass transfer in a Jeffrey fluid over a stretching sheet with heat source/sink, *Alexandria Engineering J*ournal, 52(4), 571–575.

Rasool, G., Shafiq, A., Wang, X., Chamkha, A. J. & Wakif,_A. (2024). Numerical treatment of MHD Al_2O_3–Cu/engine oil-based nanofluid flow in a Darcy–Forchheimer medium: Application of radiative heat and mass transfer laws, *International Journal of Modern Physics B*, 38(09).

Sun, Y., Dai, Y., Zhu, X., Han, R., Wang, X. & Luo, C. A. (2020). Nanocomposite prepared from bifunctionalized ionic liquid, chitosan, graphene oxide and magnetic nanoparticles for aptamer-based assay of tetracycline by chemiluminescence. Microchim, *Acta*, 63(187).

Sundaram V and Sowndhary B. B, (2025). Enhanced Thermo-Physical Properties of Titanium Dioxide Nanofluids: Applications in Renewable Energy Systems and Smart Grid Cooling Technologies. *International Conference on Electronics and Renewable Systems (ICEARS), Tuticorin, India*, 2025, 1-5.

Waheed, S. E., Galal M. Moatimid, Abeer & Elfeshawey, S. (2024). Unsteady magnetohydrodynamic squeezing Darcy-Forchheimer flow of Fe_3O_4 Casson nanofluid: Impact of heat source/sink and thermal radiation, *Partial Differential Equations in Applied Mathematics*, 10, 100666.

Wakif, A., Zaydan, M. & Sehaqui, R. (2024). Further insight into steady three- dimensional MHD Sadiadis flows of radiating- reacting viscoelastic nanofluids via Wakif's Buongiorno and Maxwell's models, *Journal of Umm Al- Qura University for Applied Sciences*, pp. 1- 13, 2024.

Wu, K., Su, D., Liu, J., Saha, R., & Wang, J. P. (2019). Magnetic Nanoparticles in Nanomedicine: A Review of Recent Advances, *Nanotechnology*, 30, 502003.

Zamani, K.M.R. & Stadler, B. J. (2020). A guideline for effectively synthesizing and characterizing magnetic nanoparticles for advancing nanobiotechnology, *a review*. *Sensors*, 20, 2554.